Cutting Force Modeling of Multi-axis Milling Processes for Variable Tool Workpiece Encounter Geometries

A.Bandil[a], T.Khot[b*], A.Guha[a], A.Tewari[a,b]

[a] Department of Mechanical Engineering, Indian Institute of Technology Bombay, Mumbai - 400 076, INDIA

[b] National Centre for Aerospace Innovation and Research, IIT Bombay, Mumbai – 400 076, INDIA

Abstract

This article describes a model for accurate prediction of cutting forces in multi-axis milling processes. It is based on analytical modeling of the interaction between the milling tool and the workpiece. The model has been developed for different milling tool geometries with several workpiece encounter profiles. The multi-axis parameters are defined using the tool lead and tilt angles relative to the workpiece surface. A mechanistic model employing the orthogonal-cutting database is used to predict cutting force coefficients which are then combined with the cutting geometry model to predict forces acting on the tool. The model has been validated against experimental cutting force data for Titanium Ti6Al4V alloy. Additionally, the model is used to simulate forces for a scenario where the cutting tool feeds into a ramped surface.

Keywords: Multi-axis milling, process modeling, tool-workpiece interaction, cutting-force prediction.

1. INTRODUCTION

Multi-axis machining processes are widely used in aerospace and related industries to produce metallic components featuring complex free-form surfaces. These components are generally precision machined within small tolerances and with high surface finish so as to meet their desired performance requirements. However, the use of difficult-to-cut materials such as Titanium and Inconel for producing such parts makes the process more challenging thus affecting overall production rates.

Five-axis milling is extensively used to produce aerospace components such as turbine blades, blisks, fuselage bulkheads and frames etc. A governing factor in milling is the generation of dynamic cutting forces in the tool-workpiece engagement region which poses limitations on the maximum metal removal rate (MRR). Higher cutting forces generally lower the permissible MRR for a given milling process, and that directly impacts the process cycle time. Additionally these cutting forces introduce vibrations into the process that lead to high frequency deflections of the spinning tool thereby affecting the accuracy of the machined surface. Cutting forces also affect the tool wear which in turn limits the number of cycles or duration for which a given tool can be used. Thus given the geometric complexity of aerospace components and the significant impact that cutting forces can have on machining processes, it is essential to mathematically model and subsequently optimize five-axis milling process parameters to achieve better part accuracies and reduced cycle times.

There is substantial scientific research that have been aimed at establishing methodologies to model cutting forces for multi-axis milling processes. Ozturk and Budak have developed models for predicting cutting forces for 5-axis ball-end milling and have studied the effect of tool orientation on cutting forces and surface roughness [1]. In a related study Ozturk, Tunc, and Budak have investigated the effect of multi-axis tool orientation on cutting force, torque, form errors and stability through modeling and experimental verification [2,3]. In another work, Budak et al. have used mathematical cutting force models as the basis for off-line feed rate scheduling to decrease overall machining time [4].

Altintas et al. have done a comprehensive review of recent developments in simulation methods for machining processes [5]. Their study also reviews algorithms for computing tool-workpiece intersections for prediction of cutting forces, torque and vibrations associated chatter. In a related work Tunc et al. have proposed an approach for integrating machining process models with CAM simulation tools for comparison of machining strategies for productivity [6].

However there exists a need for a model that can analyze and establish baseline 5-axis machining process parameters for a combination of tool and tool-workpiece encounter configurations. The work presented in this study describes the approach to model these tool-workpiece encounter combinations and simulated results for different interaction scenarios.

2. MODELING APPROACH

The methodology for mathematically modeling the cutting forces employs a mechanistic approach [7]. The basis of this approach lies in establishing an empirical relationship in which the basic orthogonal cutting parameters are estimated using regression curve-fitting of several experimental cutting test data. This empirical relationship computes cutting force coefficients which are subsequently used to determine cutting forces acting at infinitesimal line elements of a given milling tool cutting edge. The individual force components for all discretized elements are then summed up to determine the total force acting on the milling tool.

2.1 Geometric modeling of a generalized milling tool

There are several geometric features such as tool diameter; helix and rake angles, which govern the performance of the milling process. Hence these features must be modeled accurately so as to be used with the force model to predict the cutting forces.

Any milling tool geometry envelope can be modeled as function of 7 tool geometric parameters: $R, R_r, R_z, \alpha, \beta, h \; and \; D$ as shown in Fig.1
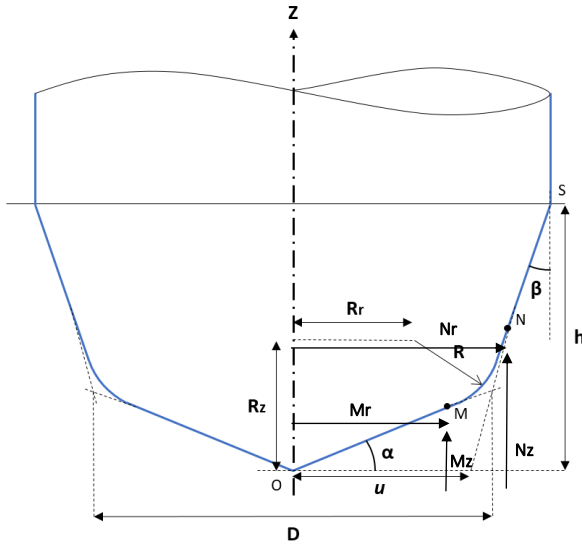

Fig. 1. Geometric parameters for a generalized milling tool model

The periphery of the tool is divided and modeled for three geometric segments: two linear taper zones *OM* and *NS*; and one Arc zone *MN*. The instantaneous radii for a given axial elevation (z) in each zone can be determined as [8]:

$$r(z) =$$

$$\begin{cases} \dfrac{z}{\tan \alpha} & \dots OM \\ \sqrt{R^2 - (R_z - z)^2} + R_r & \dots MN \\ u + z \tan \beta, where \; u = \dfrac{D}{2}(1 - \tan \alpha \tan \beta) & \dots NS \end{cases} \quad (1)$$

The radial and axial offsets of points M and N are as:

$$M_r =$$

$$\dfrac{\sqrt{(R^2 - R_z{}^2)\tan^2 \beta + 2R_z(R_r - u)\tan \beta - (R_r - u)^2 + R^2}}{\tan^2 \beta + 1} \quad (2)$$

$$M_z = M_r \tan \alpha \qquad for \; 0 \le \alpha < 90^0 \quad (3)$$

$$N_z = \dfrac{(R_r - u)\tan \beta + R_z}{\tan^2 \beta + 1} +$$

$$\dfrac{\sqrt{(R^2 - R_z{}^2)\tan^2 \beta + 2R_z(R_r - u)\tan \beta - (R_r - u)^2 + R^2}}{\tan^2 \beta + 1} \quad (4)$$

$$N_r = u + N_z \tan \beta \qquad for \; 0 \le \alpha < 90^0 \quad (5)$$

The above mathematical expressions determine the boundaries of the surface of a milling tool envelope for a given set of its 7 tool geometric parameters. Figure 2 shows the tool envelopes for 6 different tool geometries based on the above formulation.

Additionally two immersion angles are specified which determine the angular extent to which the milling tool is immersed into the workpiece volume.

The first angle is the axial immersion angle (K). It is defined as the angle between the tool axis and normal of the infinitesimal cutting edge/cutting point (see Fig. 4). This is expressed mathematically as:

$$\mathcal{K}(z) = \begin{cases} \alpha & for \; along \; line \; OM \\ sin^{-1}\left(\dfrac{r(z) - R_r}{R}\right) & for \; along \; arc \; MN \\ \dfrac{\pi}{2} - \beta & for \; along \; line \; NS \end{cases} \quad (6)$$
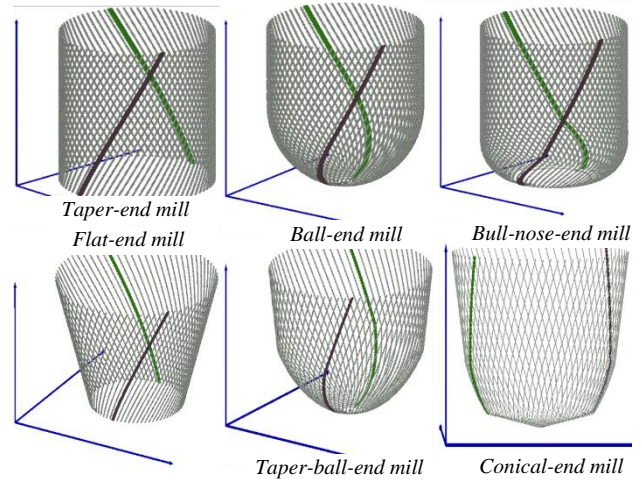

Fig. 2. Different milling tool geometries generated from the model showing cutting edge profiles

The second angle is the Radial Immersion angle, $\Phi_j(z)$, which is defined as the angular position of a point on the cutting edge in the x-y plane measured from the +y axis. This is expressed as follows:

$$\Phi_j(z) = \theta + (j - 1)\Phi_p - \Psi_j(z) \quad (7)$$

Here Φ_p is the cutting flute pitch angle defined as π/N where N is the number of cutting flutes.

$\Psi_j(z)$ is the cutting edge lag angle defined as

$$\Psi_j(z) = \dfrac{z}{R_0}\tan i_0 \quad (8)$$

where R_0 is the shank radius of the tool and i_0 is the flute helix angle.

Once the tool surface and cutting edges are defined, it is discretized into infinitesimal points in the Tool Coordinate System (TCS) as follows:

$$\begin{cases} xx_{tcs} = r(z)\sin\Phi(z) \\ yy_{tcs} = r(z)\cos\Phi(z) \\ zz_{tcs} = z \end{cases} \qquad (9)$$

To model the multi-axis rotational motion, the tool axis orientation is defined with the help of two angles. First is the lead angle (L) which is the angular rotation of tool axis about the cross feed direction (C) with respect to the surface normal (N). Second is the tilt angle (T) which is the angular rotation of tool axis about the feed direction (F) with respect to the surface normal (N). The lead and tilt angles are used to transform the coordinates of the discretized surface points from TCS to FCN. This is done using a transformation matrix as follows:

$$T = \begin{bmatrix} \cos(L) & 0 & \sin(L) \\ \sin(L)*\sin(T) & \cos(T) & -\sin(T)*\cos(L) \\ -\cos(T)*\sin(L) & \sin(T)*\sin(L) & \cos(T)*\cos(L) \end{bmatrix} \quad (10)$$

Details pertaining to tool-workpiece engagement computation can be found in references [1] and [3].

2.2 Modeling chip dimensions

Chip dimensions depend on the machining parameters such as cutting depth, feed rate, lead and tilt angles, and tool geometry (tool diameter and helix angle). The 3 main chip geometric dimension parameters are: Chip thickness; chip width; and chip length [1,3].

The chip thickness depends on cutting feed, axial immersion angle (K) and radial immersion angle (Φ). For a given surface point, the chip thickness is the component of S_t along the surface normal vector at the point as shown in Figure 3.

The normal vector of any point P on the tool surface in FCN can be written as:

$$\begin{Bmatrix} N_x \\ N_y \\ N_z \end{Bmatrix}_{FCN} = [T] \begin{Bmatrix} \sin\mathcal{K}\sin\Phi \\ \sin\mathcal{K}\cos\Phi \\ -\cos\mathcal{K} \end{Bmatrix}_{TCS} \qquad (14)$$

The chip thickness is then determined as [1,3]:

$$t_n(S_t, \Phi, \mathcal{K}) = S_t \times \frac{\overrightarrow{N_{FCN}} \cdot \overrightarrow{feed}}{|\overrightarrow{feed}|} \qquad (15)$$

where S_t is the chip thickness vector along the feed direction.

Chip width is defined as the projected length of an infinitesimal cutting element in the direction of cutting velocity. It varies as a function of $\mathcal{K}$. Chip width is expressed as a function of axial incremental value and axial immersion angle [1,3]:

$$db = \frac{dz}{\sin\mathcal{K}} \qquad (16)$$

Chip length is defined as the distance between two adjacent (along axial direction) discretized cutting points. It is expressed as:

$$ds = \sqrt{(\vec{X}(j,i) - \vec{X}(j-1,i))^2} \qquad (17)$$

$\vec{X}(j,i)$ and $\vec{X}(j-1,i)$ are position vectors of two adjacent points in TCS [1,3].
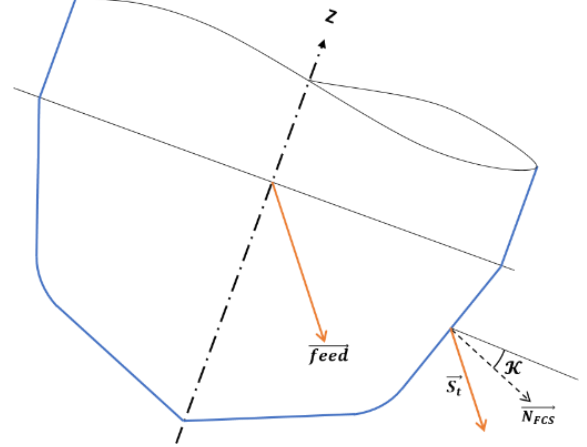

Fig. 3. Chip thickness dimension

2.3 Determining cutting forces

The forces experienced by the tool are calculated by summing the forces experienced by the individual discretized cutting elements. The force in each element is segregated into an edge force component and a cutting force component.

2.4.1 Edge force component

Edge forces arise due to rubbing or ploughing of the cutting edge on the workpiece. A coefficient is defined mechanistically using experimental data to determine the edge forces for each of the three force components: along tangential direction (K_{te}); radial direction (K_{re}); and axial direction (K_{ae}). For Titanium, the values of these coefficients are [7]:

$$K_{te} = 24N/mm;\ K_{re} = 43N/mm;\ K_{ae} \approx 0N/mm$$

2.4.2 Cutting force component

The cutting force component is the force due to shearing of the workpiece material by the cutting edge in the shear zone. Again, a coefficient is defined mechanistically using experimental data to determine the cutting forces along tangential, radial, and axial directions. These coefficients are mathematically expressed as follows:

$$\begin{cases} K_{tc} = \dfrac{\tau}{\sin\emptyset_n} \dfrac{\cos(\beta_n - \alpha_n) + \tan\eta_c \sin\beta_n \tan i}{c} \\[2mm] K_{rc} = \dfrac{\tau}{\sin\emptyset_n \cos i} \dfrac{\sin(\beta_n - \alpha_n)}{c} \\[2mm] K_{ac} = \dfrac{\tau}{\sin\emptyset_n} \dfrac{\cos(\beta_n - \alpha_n)\tan i - \tan\eta_c \sin\beta_n}{c} \end{cases} \quad (18)$$

Here $c = \sqrt{\cos^2(\phi_n + \beta_n - \alpha_n) + \tan^2\eta_c \sin^2\beta_n}$

τ is the shear stress along the shear plane.

908

Details of mathematical derivations and notations of above expressions for K_{tc}, K_{rc}, and K_{ac} can be found in reference [7].

2.4.3 Calculating cutting forces:

The elemental tangential, radial and radial force acting on the cutting edge are expressed as [1]:

$$dF_t(\theta, z) = K_{te}dS + K_{tc}t_n(\theta, \Phi, K)db$$

$$dF_r(\theta, z) = K_{re}dS + K_{rc}t_n(\theta, \Phi, K)db$$

$$dF_a(\theta, z) = K_{ta}dS + K_{ta}t_n(\theta, \Phi, K)db \quad (19)$$

In the FCN coordinate system, these forces can be expressed as:

$$\begin{Bmatrix} dF_F \\ dF_C \\ dF_N \end{Bmatrix} = [T][A] \begin{Bmatrix} dF_t \\ dF_r \\ dF_a \end{Bmatrix} \quad (20)$$

Where,

$$[A] = \begin{bmatrix} -\sin K \sin \phi & -\cos \phi & -\cos K \sin \phi \\ -\sin K \cos \phi & -\sin \phi & -\cos K \cos \phi \\ \cos K & 0 & -\sin K \end{bmatrix} \quad (21)$$

The total force acting on the tool is then determined as:

$$F_F(\theta) = \sum_{j=1}^{L_p} dF_F(\theta, z) \qquad F_C(\theta) = \sum_{j=1}^{L_p} dF_C(\theta, z)$$

$$F_N(\theta) = \sum_{j=1}^{L_p} dF_N(\theta, z)$$

$$(22)$$

Where, L_p is the total number of discretized cutting elements at a given tool angular position θ.

3. RESULTS AND DISCUSSION

The model has been validated with several cutting force experiments. The experiments were performed for Titanium Ti6Al4V alloy on a 5-axis CNC machine (DMG DMC 125FD). A solid carbide 2-fluted ball end mill (Sandvik CoroMill® Plura 1B230-1000-XA 1630) with 10 mm shank diameter was used to cut linear slots (full radial engagement) on flat plate specimens clamped on a stationary table type dynamometer (by Kistler) for real-time measurement of cutting forces.

The experiments were performed under dry conditions with the following process parameters—Spindle speed: 3000 RPM; feed: 0.08 mm/tooth-rev; and cutting depth: 0.5 mm.

Figure 5 shows a comparison between experimentally measured and modeled cutting forces Cross-feed, Feed, and Thrust directions with tool lead and tilt angles as zero. The model predictions of the cutting forces can be perceived to be fairly accurate with a deviations of approximately 5% and 10% in the Feed and Cross-feed forces respectively.
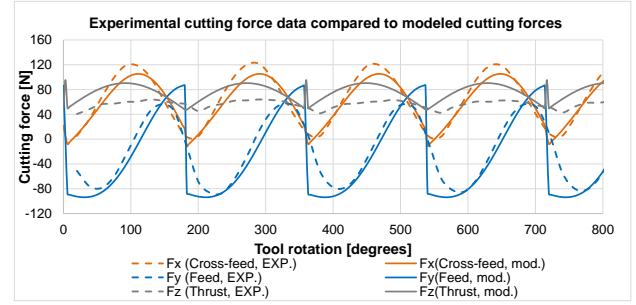

Fig.4. Comparison of experimental and modeled cutting forces

The above force model has been extended to model 9 different tool-workpiece interaction scenarios. These scenarios are combinations of the tool and workpiece orientations. As a test case, one particular scenario is described. This scenario models the cutting Tool feeding into a ramped surface. The following criterion is used to model the cutter-workpiece interaction zone:

*A given tool workpiece point **P** does not lie in the engagement region in the following conditions:*

1) *If $P_x \leq X$ and $P_z > 0$*

2) *If $P_x > X$ and $P_z > (P_x - X) \tan \alpha$*

Here P_x and P_z are the X, and Z coordinates of point **P**. X is the distance between the tool tip and start of the ramp, and α is the ramp angle.

Figure 5 shows a schematic representation of the tool workpiece engagement scenario and the variation of the cutting forces as the tool enters the ramped surface. The material and process parameters used were the same as in the model validation study discussed above. Additionally, the ramp angle α was taken as 30° and X was taken as 3mm. It can be seen from the plots that as the tool feeds into the ramped surface, the cutting forces increase monotonically. The behavior of the forces can be attributed to the effect of the tool helix angle and the ramped surface on the orientation and motion of the cutting edges within the tool-workpiece engagement zone.

4. CONCLUSIONS

In this work a method for modeling different tool-workpiece interaction scenarios particular to multi-axis end milling processes is presented. A geometric model for a generalized end mill has been used in conjunction with a mechanistic cutting force model built on regression analysis of cutting force experiments for Titanium. This is a robust model that can be utilized for performing preliminary studies during the process planning stages for various multi-axis milling operations. It provides the user a platform to model various tool geometries and workpiece interaction scenarios before performing actual experiments. Furthermore, the scope of the model can be advanced further by integrating it with models for predicting tool wear and vibrations. This model is currently undergoing validation studies, and additional material models are under development.
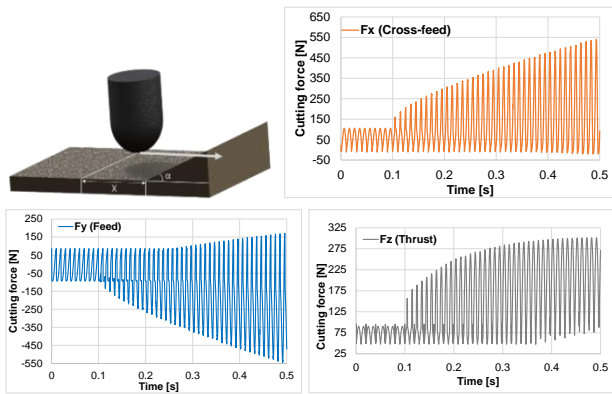
Fig. 5. Cutter-workpiece interaction scenario and cutting force profiles

ACKNOWLEDGEMENT

References

[1]   Ozturk E. and Budak E., Modelling of 5-Axis milling processes, *Machining Science and Technology,* **11** (2007) 287-311.

[2]   Ozturk E., Tunc L.T., Budak E., Investigation of lead and tilt angle effects in 5-axis ball-end milling processes, *International Journal of Machine Tools and Manufacture*, **49** (2009) 1053-1062

[3]   Budak E.,. Ozturk E., Tunc L.T., Modeling and simulation of 5-axis milling processes, *CIRP Annals*, **58** (2009) 347-350.

[4]   Budak E., Lazoglu I., Guzel B.U., Improving Cycle Time in Sculptured Surface Machining Through Force Modeling, *CIRP Annals*, **53** (2004) 103-106.

[5]   Altintas Y., Kersting P., Biermann D., Budak E., Denkena B., Lazoglu I., Virtual process systems for part machining operations, *CIRP Annals*, **63** (2014) 585-605.

[6]   Tunç L.T., Ozkirimli O., Budak E., Machining strategy development and parameter selection in 5-axis milling based on process simulations, *The International Journal of Advanced Manufacturing Technology,* **85** (2016) 1483-1500.

[7]   Budak E., Altintaş Y., Armarego E. J. A., Prediction of Milling Force Coefficients From Orthogonal Cutting Data, *Journal of Manufacturing Science and Engineering,* **118** (1996) 216-224.

[8]   Altintas Y. and Engin S., Generalized Modeling of Mechanics and Dynamics of Milling Cutters, *CIRP Annals*, **50** (2016) 25-30.